PHYSICAL REVIEW A VOLUME 13, NUMBER 1 JANUARY 1976

Hybrid theory and calculation of e-N_2 scattering

N. Chandra* and A. Temkin

Theoretical Studies Group, Goddard Space Flight Center, National Aeronautics and Space Administration, Greenbelt, Maryland 20771

(Received 24 July 1975)

A theory of electron-molecule scattering is developed which is a synthesis of close-coupling and adiabatic-nuclei theories. Specifically, the theory is close coupling with respect to vibrational degrees of freedom but adiabatic-nuclei with respect to rotation. In addition, this theory can be applied to any number of partial waves required; the remaining ones can be calculated purely in one or the other approximation. A theoretical criterion based on fixed-nuclei calculations and not on experiment can be given as to which partial waves and energy domains require the various approximations. The theory allows all cross sections (i.e., pure rotational, vibrational, simultaneous vibration-rotation, differential, and total) to be calculated. Explicit formulas for all these cross sections are given. The theory is applied to low-energy e-N_2 scattering. The fixed-nuclei results are such that the criterion shows clearly that vibrational close coupling is necessary, but only for the Π_g partial wave. The contribution of remaining partial waves can be obtained directly from the adiabatic-nuclei approximation. The close-coupling calculation for the Π_g wave is carried out, and we find that it does give rise to the substructure as well as the gross structure of the 2.4-eV resonance. When this amplitude is combined with the adiabatic amplitudes, we can compute absolute values of all cross sections of interest. In particular we find that vibrational excitation cross sections are about twice as large as previously inferred. The momentum-transfer cross section can also be computed, and it too reveals substructure within the gross structure resonance.

I. INTRODUCTION

Molecular nitrogen is a major constituent of the atmosphere to an altitude of about 500 km. Thus it can be expected that the scattering of electrons from N_2 will be an important process in the aeronomy of the atmosphere particularly above the E region, where photoionization of many of the upper atmospheric constituents by solar uv produces an abundance of electrons. For example, the resonances in the e-N_2 vibrational excitation cross sections in the vicinity of 2.4 eV have been used by Newton *et al.*[1] to explain an enhanced $O^+ + N_2(v) \rightarrow NO^+ + N$ rate which in turn will lead to the observed decrease in ambient electron density in the F_2 region during times of enhanced air glow giving rise to stable auroral red (SAR) arcs via the reaction $e + NO^+ \rightarrow N + O$.

The 2.4-eV e-N_2 resonance is known to be a very complex structure. Fortunately there is a wealth of experimental details,[2] and more or less phenomonological theories to explain them. It is important however that this complicated structure be understood from a fundamental—essentially *ab initio*—point of view, in order that researchers be able to predict scattering from other molecules which cannot be prepared in the laboratory, but which we now know to exist in many astrophysical environments.[3] We believe that the present modification and synthesis of existing theories will complete the fundamental approximations which must underlie the methodologies to be employed in such calculations.

In Sec. II we shall describe the e-N_2 2.4-eV resonance and briefly review the previous calculational theories leading to the point in Sec. III that, strictly on the basis of fixed-nuclei calculations (and not experiment) of the Π_g partial wave, one can infer that the adiabatic-nuclei theory will not suffice to describe the substructure of the resonance.[4] The fixed-nuclei calculations which are an extension of those of Burke and Chandra[5] to a series of internuclear distances R are also described in Sec. III. In Sec. IV we develop the vibrational-close-coupling theory and show that our calculations for the Π_g partial wave do reveal the substructures of this resonance as more states are added, while at the same time showing reasonable convergence when a sufficient number of states is retained. The main formulas of the adiabatic-nuclei approximation are reviewed in Sec. V; by simple inspection one may then see how to combine the vibrational-close-coupling with adiabatic-nuclei theories: the process is one of substitution of the appropriate scattering matrices of the one theory for the corresponding ones of the other.

The pseudopotential method whereby exchange and polarization have been simulated in Ref. 5, as well as its carryover in the vibrational-close-coupling portion of the present work, renders this calculation as not purely fundamental in practice. (In point of fact it depends on one adjustable parameter.) Nevertheless the manner in which one may in principle derive both exchange and polarization from an unparametrized ansatz for the total wave function has been given (cf. Refs. 15 and 16, for example); thus the one phenomenological aspect of

the present investigation should be considered an item of calculational convenience rather than in contradiction to the above description of the hybrid theory as essentially *ab initio*.

Results and comparisons with experiment are also given in Sec. V. An important aspect of the calculations is that they yield absolute normalization for individual vibrational excitation cross sections, whereas as far as we know all measurements are relative or have been done at individual angles. Furthermore the theory is complete: it gives formulas for total and differential cross sections of individual and averaged transitions for vibrational and/or rotational excitation as well as pure elastic scattering. Simultaneous vibration-rotation differential cross sections can also be calculated (although that is not done here) as well as the momentum transfer. The latter, which is calculated, is particularly interesting because it reveals substructure similar to that of the elastic scattering.

Finally in Sec. VI we give a brief discussion of how this method fits in with other methods and possible generalizations.

II. PRELIMINARIES

Experimentally the low-energy e-N_2 resonance is a complicated beast. It was first measured in detail in vibrational excitation by Schulz[6] as a series of irregular peaks (cf. Figs. 11–13). The results have been importantly complemented by the measurement of the total cross section by Golden,[7] which shows a gross structure peak centered at about 2.4 eV superimposed on top of at least five prominent subpeaks between 1.8 and 3.2 eV (cf. Fig. 7). The observed inelastic structure led in short order to its interpretation (crudely described) as a compound state of the electron and target system (i.e., the N_2^- ion[8,9]) with the substructure due to the interference between the various vibrational states of the compound system. This general physical interpretation of the structure is certainly correct; the difficulty with the calculations is that they are not *ab initio*, and thus they contain many adjustable parameters. It should be added, however, that the physical and mathematical refinements of this general approach have been greatly developed since the original papers, most successfully by Birtwistle and Herzenberg.[10] That calculation, which is based on a boomerang model, gives remarkable agreement with the shapes of the vibrational excitation curves as measured by Ehrhardt and Willmann,[11] but it too does not give absolute values.

In addition to the types of calculations mentioned above, there have been other, more *ab initio* types of investigations. One is a calculation by Krauss and Mies[12] of N_2^- as a bound-state structure. This calculation confirmed the assignment by Gilmore[13] of this resonance as a Π_g "state," and it showed that it is a shape rather than a Feshbach resonance. The calculation is truly a 15-electron self-consistent-field calculation, but since the Π_g symmetry overlaps the ordinary e-N_2 continuum, which can be of lower energy, some delicate restrictions on the variation were necessary to assure that the resonant state was not contaminated by this nonresonant scattering of the same symmetry. On that score we can all state that the calculation was in good hands with the NBS investigators.[12]

Finally, two single-center fixed-nuclei calculations have been carried out: The first by Burke and Sinfailam[14] includes full exchange of the incident and orbital electrons, but no induced polarization; the second by Burke and Chandra[5] includes polarization and simulates exchange by orthogonalizing the scattered to the bound orbitals. This "pseudopotential" approach provides the basis of all fixed-nuclei aspects of the present calculation, and we shall discuss it as appropriate in succeeding sections.

III. FIXED-NUCLEI THEORY AND CALCULATIONS

In contrast to its application in bound-state problems, the fixed-nuclei approximation for electron-molecule scattering[15,16] assumes not only that the nuclei are fixed (at a distance R apart), but that the target molecular wave function $\Phi(x;R)$ has been precalculated at each, in principle, arbitrary, internuclear separation R. As a result the scattering associated with a total wave function ($\vec{r}$ is the coordinate of the scattered and x_i those of the orbital electrons)

$$\Psi^{(m)} = \psi_m(\vec{r};\vec{R})\Phi(x_i;R) \tag{3.1}$$

exhibits no particular stationary properties with respect to variations of R about the equilibrium separation of the target molecule $R=R_0$. This is very forcefully exhibited here, when we extend the calculations at the equilibrium separation[5] ($R=R_0=2.068a_0$) to four additional values of R of the N_2 wave function given by Nesbet[17]: $R=1.744\,393$, $1.868, 2.268, 2.391\,607$.

To review the fixed-nuclei calculation (cf. Ref. 5 but our notation is somewhat different), the ground state $^1\Sigma_g^+$ of N_2 is a closed shell described by a single Slater determinant

$$\Phi = \det(\phi_{\alpha_1}(x_1)\phi_{\alpha_2}(x_2)\cdots\phi_{\alpha_{14}}(x_{14})), \tag{3.2}$$

where the α_i can readily be identified from the configuration $1\sigma_g^2\,2\sigma_g^2\,3\sigma_g^2\,1\sigma_u^2\,2\sigma_u^2\,1\pi_u^4$ of the ground ($^1\Sigma_g^+$) state of N_2. The bound-state function[17] which

is an LCAO function—meaning pairs of orbitals are centered about the separate nuclei— is converted to a single-center basis using a program of Faisal and Tench[18]:

$$\phi_\alpha(\vec{r}) = \sum_{l\geq\lambda_\alpha}{}'' \frac{1}{r}\phi_l{}^\alpha(r)Y_{l\lambda_\alpha}(\Omega)\,. \tag{3.3}$$

(A double prime indicates every second term is to be taken. The coordinate x includes spin variables plus the vector $\vec{r}$.) A similar expansion is now made of the scattered orbital[16]

$$\Psi_m(\vec{r};\vec{R}) = \sum_{l_i l_j}\frac{u^{(m)}_{l_i l_j}}{r}Y_{l_i m}(\Omega)Y^*_{l_j m}(\Omega_0)\,, \tag{3.4}$$

where Ω_0 are the sperical angles of the internuclear axis in the laboratory frame and $r=(r,\Omega)$, i.e., unprimed coordinates are the coordinates in the molecular frame.

With the use of (3.3) the static potential seen by the scattered electron is naturally expanded in single-center coordinates (in rydberg units)

$$\left\langle\Phi\left|\frac{2Z}{|\vec{r}-\vec{R}/2|}+\frac{2Z}{|\vec{r}+\vec{R}/2|}-\sum_{i=1}^{N}\frac{2}{|\vec{r}-\vec{r}_i|}\right|\Phi\right\rangle = \sum_\lambda{}'' V_\lambda(r)P_\lambda(\cos\theta)\,. \tag{3.5}$$

The equations satisfied are then derived from the variational principle:

$$\delta\int\Psi^{(m)*}(H-E)\Psi^{(m)}\,d\tau = 0\,, \tag{3.6a}$$

which is equivalent to the projection

$$\int Y^*_{l_i m}Y_{l_j m}(H-E)\Psi^{(m)}d\tau' = 0\,, \tag{3.6b}$$

where $d\tau'$ means integration over all coordinates but r (including integration over Ω_0). In practice this set of coupled equations, which may readily be derived from (3.1)–(3.5), is augmented to include an induced polarization potential

$$V^{(\mathrm{pol})}(\vec{r};R) = -\left(\frac{\alpha_0(R)}{r^4}+\frac{\alpha_2(R)}{r^4}P_2(\cos\theta)\right)(1-e^{-(r/r_0)^6})\,, \tag{3.7}$$

The calculation[5] also includes orthogonality to all occupied orbitals of the same symmetry via Lagrange multipliers. The equations satisfied by $u^{(m)}_{l_i l_j}(r)$ of Eq. (3.4) are then

$$\left(\frac{d^2}{dr^2}-\frac{l_i(l_i+1)}{r^2}+k^2\right)u^{(m)}_{l_i l_j}(r) - \sum_{l_j} v^{(m)}_{l_i l_j}(r)\,u^{(m)}_{l_j l_i}(r) = \sum_\alpha \lambda_\alpha\phi^{(\alpha)}_{l_i}(r)\,, \tag{3.8}$$

where

$$v^{(m)}_{l_i l_j} = \sum\left(\frac{2l_j+1}{2l_i+1}\right)^{1/2}(l_j\lambda 00\,|\,l_i 0)(l_j\lambda m 0\,|\,l_i m)v_\lambda(r) \tag{3.9}$$

and

$$v_\lambda(r) = V_\lambda(r)+V^{(\mathrm{pol})}_\lambda(r)\,. \tag{3.10}$$

$V^{(\mathrm{pol})}_\lambda$ are the multiple components of $V^{(\mathrm{pol})}$ from (3.7), thus in particular $V^{(\mathrm{pol})}_\lambda = 0$ for $\lambda > 2$. [The remaining symbols in (3.9) are Clebsch-Gordan coefficients.]

The calculation for each R was done just as the calculations of Burke and Chandra[5] at $R=R_0$. One only needs the dependence of the polarizabilities on R. These were taken of the form

$$\alpha_0(R) = 12.0+1.692(R-R_0)\,, \tag{3.11a}$$

$$\alpha_2(R) = 4.2+2.031(R-R_0)\,. \tag{3.11b}$$

Equations (3.11) were chosen to give the correct polarizabilities at $R=R_0$ and to reduce correctly to the united atom limit: $\alpha_0(0)$ $(=\alpha_{\mathrm{silicon}}) = 8.5a_0^3$ and $\alpha_2(0)=0$. The value $8.5a_0^3$ was interpolated from Sternheimer's[19] calculation of the polarizabilities of Cl^-, K^+, and Ca^{++}. It is to be noted that Eqs. (3.11) are somewhat different from Truhlar[20] who used Raman data to get an accurate estimate of the derivatives in the neighborhood of $R=R_0$. Our own interpolations, while somewhat cruder, should apply over a larger range in R, and thus be more suitable to excitation of higher-lying vibrational states. Finally the value of r_0 was retained at 1.592 as independent of R. That value was chosen,[5] so that the Π_g resonance for $R=R_0$ occured at exactly $k^2=2.394$ eV.

The scattering is determined from the asymptotic solution of (3.8):

$$\lim_{r\to\infty}u^{(m)}_{l_i l_j} = k^{-1/2}\left[\sin(kr-\tfrac{1}{2}\pi l_i)\,\delta_{l_i l_j} + K^{(m)}_{l_i l_j}\cos(kr-\tfrac{1}{2}\pi l_j)\right]. \tag{3.12}$$

The K matrix as indicated in (3.12) is diagonal in m; it is also real, symmetric, and for homonuclear targets connects only l_i and l_j of the same parity. In matrix notation the scattering is naturally expressed in terms of a matrix proportional to the T matrix. In Ref. 5 this matrix is taken to be $\underline{T}^{(m)}$ which is related to $\underline{K}^{(m)}$ by

$$\underline{T}^{(m)} = 2i(1-i\underline{K}^{(m)})^{-1}\underline{K}^{(m)}\,. \tag{3.13}$$

In Ref. 16, which gives the original derivation of the coupled fixed-nuclei cross sections (using a spherical analysis), the scattering is written in terms of the a matrix which is related to the above T matrix by[21]

$$a_{l_i l_j m} = i^{l_i-l_j-1}\{[\pi(2l_j+1)]^{1/2}/k\}\,T^{(m)}_{l_i l_j}\,. \tag{3.14}$$

The fixed-nuclei results are most conveniently given in terms of the sum eigenphase shifts. The eigenphases are the arctangents of the eigenvalues of the K matrix:

$$\det\left|\underline{K}^{(m)} - \lambda^{(m)}\underline{I}\right| = 0 , \tag{3.15a}$$

$$\Delta^{(m)} = \sum_i \tan^{-1}\lambda_i^{(m)} , \tag{3.15b}$$

where the sum in (3.15b) goes over all coupled states that are included (and is found to converge with inclusion of approximately eight coupled states) $\underline{I}$ is the unit matrix. In Table I we give a selection of our results for Σ_g, Σ_u, Π_u partial waves as a function of internuclear separation R. The $R(=R_0)=2.068$ results are just those of Burke and Chandra.[5] A detailed description of that generic program has been published by one of us,[22] and that program is what was applied here.

We also note in addition to $m=0,1,\ldots$ corresponding to $\Sigma,\Pi,\ldots$ that the parity of the index l (even or odd corresponding to g or u) is also a good quantum number as well as the spin S. The latter is always $S=\frac{1}{2}$ corresponding to doublet multiplicity, since N_2 is a closed-shell ($^1\Sigma_g$) target. (We therefore suppress the doublet label, for example, $^2\Pi_g$, on our partial wave notation.)

The sum of eigenphases for non-Π_g phase shifts are seen to change minimally as a function of R (although it is interesting that for Σ_g the minute change is an oscillatory one). The change is also slow and smooth as a function of the impacting energy k^2. For those partial waves, therefore, the adiabatic-nuclei theory for both rotational and vibrational excitation applies (see below).

On the other hand the change with both R and k^2 of the Π_g wave, given in Fig. 1, is dramatic! As a function of k^2 the salient feature is the resonant behavior. If one confines attention to the equilibrium separation R, one[5] evaluates the width $\Gamma \cong 0.4$ eV, which is sensibly larger than the vibrational spacing $\Delta E_v \cong 0.29$ eV. It was for this reason that we previously believed the adiabatic nuclei theory would be at least semiquantitatively applicable to that partial wave as well.[23] However, if one looks at the curves for $R>R_0$ then one sees that the resonance has diminished to $\Gamma \cong 0.14$ eV for $R=2.391\,607$. And even at $R=2.268$, $\Gamma \cong 0.25$ eV which is smaller than the vibrational spacing of N_2; in other words the time ($\tau \propto \Gamma^{-1}$) spent by the incoming electron in the vicinity of the molecule is comparable to or longer than the vibrational period of the nuclei. This is a definite violation of a basic criterion for the validity of the adiabatic-nuclei theory, and it gives a purely theoretically determined basis for distrusting the adiabatic-nuclei theory for this partial wave.[24] We therefore turn in Sec. IV to vibrational close coupling and its amalgamation into the adiabatic-nuclei theory.

Before concluding this section, we give in Fig. 2 a comparison of our fixed-nuclei width and position curves versus R as compared to the calculations of Krauss and Mies[12] and Birtwistk and Herzenberg.[10] Considering the different natures of these calculations, we consider the agreement to be remarkable.

IV. VIBRATIONAL CLOSE COUPLING

It is clear from the foregoing that it is necessary to include the dynamical response of the nuclei to their vibrational motion. The most natural way of doing that in quantum mechanics is to expand the wave function in terms of the eigenfunctions of the vibrational motion: this is what is meant by a vibrational close-coupling expansion:

$$\Psi_{cc}^{(m)} = \Phi(x_i;R)\sum_v F_v^{(m)}(\vec{r})\chi_v(R) . \tag{4.1}$$

[The contrast of this with (3.1) should be noted.] Let us write the total Hamiltonian (in rydbergs)

$$H = H_0(R) - \nabla_r^2 - (1/M)\nabla_R^2 + V_{ee} + V_{Ne} , \tag{4.2}$$

where $H_0(R)$ is the Hamiltonian of the target molecule, with nuclei fixed at a distance R apart, and M their reduced mass. V_{ee} and V_{Ne} are the interaction potentials of the scattered electron with the orbital electrons and nuclei, respectively;

$$V_{ee} = \sum_{i=1}^{N} \frac{2}{|\vec{r}-\vec{r}_i|} , \tag{4.3}$$

$$V_{Ne} = -2Z\left(\frac{1}{|\vec{r}-\vec{R}/2|} + \frac{1}{|\vec{r}+\vec{R}/2|}\right) . \tag{4.4}$$

We derive coupled equations for the functions $F_v(\vec{r})$ in the usual way; obtaining

$$(-\nabla_r^2 - k_{v'}^2)F_{v'}(\vec{r}) + \sum_v \langle \Phi v' \left| V_{ee} + V_{Ne} \right| \Phi v\rangle_{R,x_i} F_v(\vec{r}) = 0 . \tag{4.5}$$

In deriving (4.5) one uses the conservation of energy

$$E - E_0 = k^2 + \epsilon_0 = k_v^2 + \epsilon_v , \tag{4.6}$$

where E_0 is the electronic energy of the target state satisfying the target Schrödinger equation

$$H_0(R)\Phi(x_i,R) = E_0(R)\Phi(x_i,R) . \tag{4.7}$$

One also uses the *approximation* that the rotational kinetic energy is negligible compared to its vibrational energy, so that

$$\nabla_R^2 \to \frac{1}{R}\frac{d^2R}{dR^2} \tag{4.8}$$

TABLE I. Nonresonant eigenphase sums as a function of R (mod π).

Energy (eV)	Partial wave[a]	Internuclear separation R (in units of a_0) 1.744 393	1.868	2.068	2.268	2.391 607
0.20	A	−0.1921	−0.1906	−0.1985	−0.1902	−0.1926
	B	−0.0253	−0.0645	−0.0037	0.0011	0.0038
	C	0.0351	0.0295	0.0288	0.0278	0.0271
0.40	A	−0.2960	−0.2938	−0.3048	−0.2940	−0.2972
	B	−0.0366	−0.0113	−0.0090	−0.0020	0.0012
	C	0.0503	0.0423	0.0406	0.0390	0.0379
0.60	A	−0.3772	−0.3747	−0.3878	−0.3750	−0.3787
	B	−0.0505	0.0211	−0.0202	−0.0115	−0.0083
	C	0.0572	0.0474	0.0448	0.0427	0.0411
0.80	A	−0.4450	−0.4421	−0.4570	−0.4426	−0.4467
	B	−0.0673	−0.0346	−0.0353	−0.0253	−0.0223
	C	0.0591	0.0479	0.0442	0.0414	0.0394
1.00	A	−0.5037	−0.5006	−0.5170	−0.5012	−0.5056
	B	−0.0845	−0.0503	−0.0530	−0.0419	−0.0393
	C	0.0573	0.0449	0.0401	0.0368	0.0343
1.20	A	−0.5555	−0.5524	−0.5702	−0.5530	−0.5577
	B	−0.1033	−0.0677	−0.0723	−0.0603	−0.0581
	C	0.0528	0.0394	0.0337	0.0298	0.0270
1.40	A	−0.6022	−0.5989	−0.6180	−0.5997	−0.6047
	B	−0.1229	−0.0862	−0.0927	−0.0799	−0.0782
	C	0.0466	0.0323	0.0256	0.0212	0.0181
1.60	A	−0.6446	−0.6412	−0.6616	−0.6423	−0.6475
	B	−0.1428	−0.1054	−0.1137	−0.1003	−0.0990
	C	0.0389	0.0239	0.0163	0.0114	0.0081
1.80	A	−0.6835	−0.6801	−0.7018	−0.6814	−0.6869
	B	−0.1630	−0.1250	−0.1352	−0.1211	−0.1203
	C	0.0303	0.0146	0.0062	0.0009	−0.0027
2.00	A	−0.7193	−0.7158	−0.7388	−0.7176	−0.7234
	B	−0.1833	−0.1448	−0.1568	−0.1421	−0.1417
	C	0.0210	0.0046	−0.0045	−0.0102	−0.0139
2.20	A	−0.7524	−0.7480	−0.7733	−0.7514	−0.7575
	B	−0.2035	−0.1647	−0.1784	−0.1632	−0.1632
	C	0.0113	−0.0058	−0.0155	−0.0216	−0.0255
2.40	A	−0.7833	−0.7799	−0.8056	−0.7830	−0.7896
	B	−0.2235	−0.1845	−0.1999	−0.1843	−0.1846
	C	0.0011	−0.0165	−0.0269	−0.0332	−0.0373
2.60	A	−0.8122	−0.8089	−0.8359	−0.8129	−0.8198
	B	−0.2434	−0.2043	−0.2213	−0.2051	−0.2058
	C	−0.0092	−0.0274	−0.0383	−0.0450	−0.0491
2.80	A	−0.8393	−0.8361	−0.8646	−0.8409	−0.8484
	B	−0.2631	−0.2239	−0.2424	−0.2258	−0.2268
	C	−0.0197	−0.0383	−0.0498	−0.0567	−0.0609
3.00	A	−0.8649	−0.8617	−0.8917	−0.8677	−0.8756
	B	−0.2825	−0.2432	−0.2633	−0.2462	−0.2474
	C	−0.0302	−0.0493	−0.0613	−0.0684	−0.0726
3.20	A	−0.8890	−0.8860	−0.9175	−0.8929	−0.9015
	B	−0.3016	−0.2623	−0.2838	−0.2664	−0.2678
	C	−0.0408	−0.0603	−0.0727	−0.0800	−0.0841
3.40	A	−0.9119	−0.9090	−0.9418	−0.9174	−0.9265
	B	−0.3204	−0.2812	−0.3041	−0.2862	−0.2878
	C	−0.0513	−0.0712	−0.0839	−0.0914	−0.0955

TABLE I. *(continued)*

Energy (eV)	Partial wave[a]	Internuclear separation R (in units of a_0) 1.744 393	1.868	2.068	2.268	2.391 607
3.60	A	−0.9337	−0.9307	−0.9654	−0.9408	−0.9505
	B	−0.3389	−0.2997	−0.3239	−0.3056	−0.3074
	C	−0.0617	−0.0819	−0.0950	−0.1026	−0.1067
3.80	A	−0.9544	−0.9516	−0.9880	−0.9633	−0.9737
	B	−0.3570	−0.3180	−0.3434	−0.3247	−0.3266
	C	−0.0720	−0.0925	−0.1059	−0.1136	−0.1177
4.00	A	−0.9743	−0.9716	−1.0096	−0.9850	−0.9961
	B	−0.3749	−0.3359	−0.3625	−0.3434	−0.3454
	C	−0.0821	−0.1030	−0.1167	−0.1244	−0.1284
4.50	A	−1.0203	−1.0181	−1.0605	−1.0363	−1.0491
	B	−0.4179	−0.3792	−0.4087	−0.3884	−0.3907
	C	−0.1067	−0.1283	−0.1425	−0.1502	−0.1541
5.00	A	−1.0620	−1.0605	−1.1073	−1.0838	−1.0984
	B	−0.4589	−0.4204	−0.4525	−0.4311	−0.4332
	C	−0.1302	−0.1522	−0.1669	−0.1745	−0.1779

[a] Rows A, B, C refer to Σ_g, Σ_u, Π_u eigenphase sums, respectively.

and the fact

$$\left(-\frac{1}{M}\frac{1}{R}\frac{d^2R}{dR^2}+\langle\Phi(x_i,R)\,|H_0(R)\,|\,\Phi(x_i,R)\rangle_i-\epsilon_v\right)\chi_v(R)=0\,. \tag{4.9}$$

In (4.5) and (4.9) the subscripts on $\langle\ \rangle$ indicate the coordinates over which one integrates. Note in particular that $\langle\Phi v'\,|\,V_{ee}\,|\,\Phi v\rangle_{R,r_i}$ *includes the parametric dependence* of Φ on R and is therefore *not*

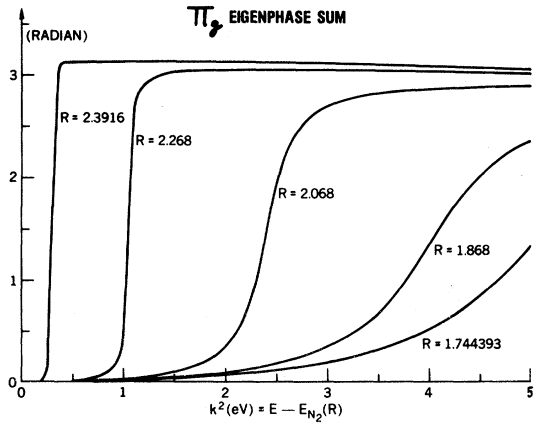

FIG. 1. Fixed-nuclei Π_g eigenphase sum (mod π) for different internuclear separations. Note that k^2 is relative to the ground-state energy of N_2 which is itself a function R; cf. bottom curve, Fig. 2.

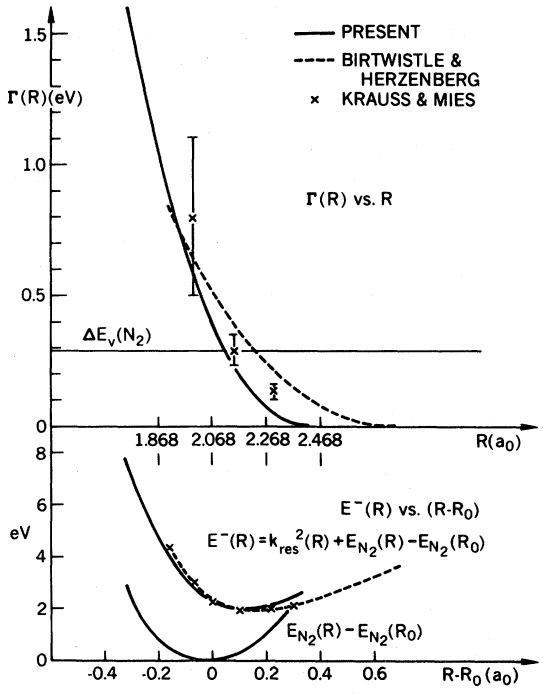

FIG. 2. Width and position of Π_g resonance vs R. The other results are from Birtwistle and Herzenberg (Ref. 10) and Krauss and Mies (Ref. 12). The lowest curve is $E_{N_2}(R)-E_{N_2}(R_0)$.

simply $\delta_{vv'}\langle\Phi|V_{ee}|\Phi\rangle_{r_i}$. On the other hand, it is true that

$$\langle\Phi v'|V_{Ne}|\Phi v\rangle_{R,x_i}=\langle v'|V_{Ne}|v\rangle_R \tag{4.10}$$

since Φ is normalized for each R and V_{Ne} is independent of $\vec{r}_i$. The net results is that the set of equations (4.5) is seen to be a set of equations purely in $\vec{r}$.

Note in deriving (4.5) we have neglected the action of ∇_R^2 on $\Phi(\vec{r}_i;\vec{R})$. This is in complete analogy with what one does in the full Born-Oppenheimer approximation wherein the equation for the vibrational wave function is derived neglecting the operation of ∇_R^2 on the parametric dependence of Φ on R [cf. specifically Eq. (4.9) above]. In the present case the purely vibrational function $\chi_v(R)$ is replaced by a close-coupling expansion $\sum_v F_v(\vec{r})\chi_v(R)$ which, as opposed to the bound-state ansatz, is seen to depend on the scattered electron's coordinates. Nevertheless the same prescription applies; ∇_R^2 operates only on that sum. The result however is quite different; the vibrational equation is automatically satisfied, Eq. (4.9), and one is left with coupled equations for the F_v, Eqs. (4.5). The ansatz (4.1) also seems to single out the electronic coordinate of the scattered electron $\vec{r}$ and treat it differently from the bound orbitals described by $\vec{r}_i$. Formally speaking, however, this lack of symmetry can be readily removed by antisymmetrizing $\Psi_{cc}^{(m)}$ of (4.1) between $\vec{r}$ and the remaining $\vec{r}_i$. In practise we shall not do this but simulate it with the same pseudopotential of the fixed-nuclei part of the calculation, $V^{(\mathrm{pol})}$ of Eq. (3.7), albeit treating it consistently with the close coupling method. In order that polarization as well as exchange be included, the *ab initio* ansatz would require, according to the method of Refs. 15 and 16, that (4.1) be augemented to read

$$\Psi_{ccpo}^{(m)}=\mathcal{A}\left((\Phi+\Phi^{(\mathrm{pol})})\sum_v F_v^{(m)}\chi_v\right). \tag{4.1'}$$

The essential item in all these treatments, as in the Born-Oppenheimer approximation for bound states, is that whereas nuclear kinetic-energy effects associated with Φ (or $\Phi+\Phi^{(\mathrm{pol})}$) can be neglected, they cannot be neglected for the coefficient functions which multiply the Φ's in the total wave function, and the potential-energy effects of all terms must be included.

To eliminate the angular dependence, we make the usual type spherical harmonic expansion. As opposed to (3.4), however, we here suppress the dependence on Ω_0, since this does not alter the dynamical equations. Let

$$F_v^{(m)}(\vec{r})=\frac{1}{r}\sum_l f_{vl}^{(m)}(r)Y_{lm}(\Omega)\,, \tag{4.11}$$

$$\langle\Phi|V_{ee}+V_{Ne}|\Phi\rangle_{x_i}=\sum_\lambda V^{(\lambda)}(r,R)P_\lambda(\cos\theta)\,. \tag{4.12}$$

The latter implies that

$$\langle\Phi v'|V_{ee}+V_{Ne}|\Phi v\rangle_{R,x_i}=\sum_\lambda V_{v'v}^{(\lambda)}(r)P_\lambda(\cos\theta)\,, \tag{4.13}$$

where

$$V_{v'v}^{(\lambda)}(r)=\langle v'|V^{(\lambda)}(r,R)|v\rangle_R\,. \tag{4.14}$$

Using all these plus the well-known formula for the integral of three spherical harmonics[25]

$$\int Y_{l'm}^* P_\lambda Y_{lm}\,d\Omega=(-1)^m[(2l+1)(2l'+1)]^{1/2}\times\begin{pmatrix}l' & \lambda & l\\ m & 0 & -m\end{pmatrix}\begin{pmatrix}l' & \lambda & l\\ 0 & 0 & 0\end{pmatrix}, \tag{4.15}$$

one can reduce (4.5) to the coupled equations

$$\left(\frac{d^2}{dr^2}-\frac{l'(l'+1)}{r^2}+k_{v'}^2\right)f_{v'l'}^{(m)}(r)=\sum_{v,l,\lambda}[(2l+1)(2l'+1)]^{1/2}(-1)^m\begin{pmatrix}l' & \lambda & l\\ m & 0 & -m\end{pmatrix}\begin{pmatrix}l' & \lambda & l\\ 0 & 0 & 0\end{pmatrix}\mathcal{U}_{v'v}^{(\lambda)}(r)f_{vl}^{(m)}(r)\,. \tag{4.16}$$

Equation (4.16) shows that the price we have to pay to get rid of the angles in (4.5) is the l coupling. In addition to that we have the summation over λ which comes from the single-center spherical expansions of V_{ee} and V_{Ne}, Eqs. (4.3) and (4.4). Finally, however, in the spirit of our fixed-nuclei calculation we include an additional pseudopotential to describe and simulate the effects of polarization and exchange. [Note, like (3.1), (4.1) is also not antisymmetrized between $\vec{r}$ and $\vec{r}_i$ $(i=1,2,\ldots,N)$.]

However the way to do is now clear: to $V_{v'v}^{(\lambda)}(r)$ we add a polarization potential gotten from appropriate matrix elements of $V^{(\mathrm{pol})}(\vec{r},R)$ of (3.7), i.e., in (4.5) we augment the potential by $\langle\Phi v'|V^{(\mathrm{pol})}|\Phi v\rangle$; this induces a change in the potential $V_{v'v}^{(\lambda)}$ of (4.14) to $\mathcal{U}_{v'v}^{(\lambda)}(r)$ in Eq. (4.16), where

$$\mathcal{U}_{v'v}^{(\lambda)}=V_{v'v}^{(\lambda)}(r)+\langle v'|V_\lambda^{(\mathrm{pol})}|v\rangle_R \tag{4.17}$$

and $V_\lambda^{(\mathrm{pol})}$ is the λth multiple component of $V^{(\mathrm{pol})}$ [see below Eq. (3.10)].

Equations (4.16) are solved in analogous fashion to (3.8); specifically here one demands the asymptotic form

$$\lim_{r\to\infty} f^{(m)}_{v'l'}(r) = [1/(k_v)^{1/2}][\sin(k_v r - \tfrac{1}{2}\pi l')\delta_{vv'}\delta_{ll'} + K^{(m)}_{v'l',vl}\cos(k_v r - \tfrac{1}{2}\pi l)]. \tag{4.18}$$

From the $K^{(m)}$ matrix one can, in analogy with (3.10) and (3.11), develop a $T^{(m)}$ and $\mathfrak{a}^{(m)}$ matrix

$$T^{(m)}_{v'l',vl} = 2i\sum_{v'',l''}[(1-iK)^{-1}]_{v'l',v''l''}K^{(m)}_{v''l'',vl}, \tag{4.19}$$

$$\mathfrak{a}^{(m)}_{v'l',vl} = i^{l'-l-1}[\pi(2l+1)/k_v k_{v'}]^{1/2}T^{(m)}_{v'l',vl}. \tag{4.20}$$

The actual calculation, as we have indicated, need only be done for the Π_g partial wave. For this partial wave there is no orthogonality requirement; on the other hand the multiplicity of coupling (v, l, and λ) makes it impossible, even on our machine (IBM 360-91), to include a sufficient number of terms to get full convergence in all coupling indices. We have therefore chosen to delimit the l coupling to three terms ($l = 2,4,6$). The λ expansion is thereby automatically restricted to seven terms ($\lambda = 0, 2, \ldots, 12$). Within this approximation we seek convergence in v. The role of the polarization potential $V^{(\mathrm{pol})}$, specifically the cutoff r_0 here will hopefully serve, in addition to exchange, to simulate the unincluded l and λ components. It was chosen so that with the inclusion of only one vibrational state, the resonance in the $v = 0 \to v' = 0$ cross section occured at $k_0^2 = 2.4$ eV (cf. Fig. 4).

We shall not dwell on the numerical aspects of this calculation: sufffice it to say that the generic program of Ref. 22 was applicable with only minor additions to (4.16). The static potentials $V^{(\lambda)}_{v'v}(r)$ were generated numerically from Nesbet's wave functions[17]; a selection of these potentials as a function of r is shown in Fig. 3. There diagonal potentials are compared with the fixed nuclei (static) potentials $V^{(\lambda)}(r, R_0)$ wherein we see that both potentials get increasingly more sharply peaked and concentrated around $r = \frac{1}{2}R_0$, but that for corresponding λ the close-coupling potentials are softer and without cusps. The off-diagonal potentials have no real counterpart in the adiabatic-nuclei theory, and they are mathematically the source of the substructure of the Π_g resonance.

To see how this substructure appears we show in Fig. 4 the Π_g contribution to the $v = 0 \to v' = 0$ cross section. The cross section is plotted for different numbers of vibrational states retained in the expansion. In addition we have shown two sets of curves, one includes two coupled $l (l = 2,4)$ components in (4.16) and one set includes three l's (2,4,6). For each case we include all λ allowed by vector coupling.

One can see that one v-term result does indeed exhibit a resonance at $k^2 = 2.4$ eV. It was essential to get this resonance that the polarization potential be included along with the static potential in $V^{(\lambda)}$. To get the resonance at the desired potition we had to choose $r_0 = 1.496$, 1.554 for two and three l-coupled calculations, respectively. These values are gratifyingly close to the value needed in the fixed-nuclei calculation 1.597.[5] Thereafter one sees as the fundamental result of this paper that the substructure begins to appear, and that by the time we have coupled in 10 and 9 vibrational states, respectively, reasonable (but not precision) convergence is seen to occur. (The program correctly includes whether various vibrational channels are energetically closed or open.) The comparison of the two-vs-three coupled l solutions shows that detailed effects do depend on the number of l's retained. Thus to obtain the second rather than the first bump as dominant in σ_{00} as is revealed by experiment (cf. Fig. 13), the retention of three l's is necessary. It is also clear that the inclusion of even more l's would be necessary to obtain the totality of peaks in the substructure. (We shall see other manifestations of the truncated substructure in other cross-section data as well.)

In Figs. 5 and 6 we give similar results for the (Π_g contribution) to $v = 0 \to 1$ and $v = 0 \to 2$ cross sections. The same type of convergence and l-coupling effects are apparent, except that the necessity of more l coupling (and consequently more v coupling) becomes progressively greater, as one goes to higher v'.

We also state for the record that the substructure does *not* appear if we retain only one l. Nor does it occur in the adiabatic-nuclei approximation[23] (see below).

V. ADIABATIC-NUCLEI APPROXIMATION, HYBRID-THEORY RESULTS

The adiabatic-nuclei approximation[26] gives the transition amplitude between vibrational rotational states $\Gamma \to \Gamma'$ as

$$f_{\Gamma'\Gamma}(\xi,\Omega') = \langle\Gamma'|f(\xi,\Omega')|\Gamma\rangle_\xi + \epsilon, \tag{5.1}$$

where $f(\xi,\Omega')$ is the fixed-nuclei amplitude with nuclear coordinates frozen at ξ. Although the error term ϵ on the right-hand side of (5.1) has never been completely elucidated, the present calculation will show that the delay time of scattering must be small compared to the period $\tau \cong \hbar_i/\Delta E_{\Gamma'\Gamma}$ associated with the largest energy quantum number of Γ

which changes to the transition (we assume $\Gamma' \neq \Gamma$), in order for ϵ to be negligible. The fixed-nuclei amplitude for scattering from a diatomic molecule is such the angular integrations in (5.1) can be done analytically,[27] whereas the integrations over R are necessarily numerical.

The resulting formula for the simultaneous rotation-vibration differential cross section (when the target is a Σ_g^+ state) can be written[28]

$$\frac{d\sigma_{j'v;jv}}{d\Omega'} = \frac{k_{j'v'}}{k_{jv}} \frac{1}{4\pi} \sum_L A_L(j'v';jv) P_L(\cos\theta') , \tag{5.2a}$$

where

$$A_L(j'v';jv) = (2L+1)(2j'+1)\sum (-1)^{l_j+\lambda_j+m+\mu}[(2l_i+1)(2\lambda_i+1)]^{1/2} a_{l_i l_j m}(v'v) a^*_{\lambda_i \lambda_j \mu}(v'v) \begin{pmatrix} l_i & \lambda_i & L \\ 0 & 0 & 0 \end{pmatrix} \begin{pmatrix} l_j & \lambda_j & L \\ 0 & 0 & 0 \end{pmatrix}$$
$$\times \sum_J (-1)^J \begin{pmatrix} l_i & l_j & J \\ m & -m & 0 \end{pmatrix} \begin{pmatrix} \lambda_i & \lambda_i & J \\ \mu & -\mu & 0 \end{pmatrix} \begin{pmatrix} j' & j & J \\ 0 & 0 & 0 \end{pmatrix}^2 \begin{Bmatrix} l_i & \lambda_i & L \\ \lambda_j & l_j & J \end{Bmatrix} (2J+1) , \tag{5.2b}$$

and for joint vibration-rotational excitation[29]

$$a_{l_i l_j m}(v', v) = \int_0^\infty \chi_{v'}(R) a_{l_i l_j m}(R) \chi_v(R) R^2 \, dR . \tag{5.3}$$

If one averages over initial rotational states j and sums over final states j', one arrives at

$$\frac{d\sigma_{v',v}}{d\Omega'} = \frac{k_{v'}}{k_v} \frac{1}{4\pi} \sum_L A_L(v', v) P_L(\cos\theta') , \tag{5.4a}$$

where the rotationally averaged coefficients are

$$A_L(v', v) = (2L+1) \sum [(2l_i+1)(2\lambda_i+1)]^{1/2} a_{l_i l_j m}(v', v) a^*_{\lambda_i \lambda_j \mu}(v', v)$$
$$\times \begin{pmatrix} l_i & \lambda_i & L \\ 0 & 0 & 0 \end{pmatrix} \begin{pmatrix} l_j & \lambda_j & L \\ 0 & 0 & 0 \end{pmatrix} \begin{pmatrix} l_i & \lambda_i & L \\ m & \mu & -(m+\mu) \end{pmatrix} \begin{pmatrix} l_j & \lambda_j & L \\ m & \mu & -(m+\mu) \end{pmatrix} . \tag{5.4b}$$

The total cross sections are quite obviously just 4π times the $L = 0$ terms of the respective expressions,

$$\sigma_{j'v',jv} = (k_{j'v'}/k_{jv}) A_0(j'v';jv) , \tag{5.5}$$

$$\sigma_{v',v} = \frac{k_{v'}}{k_v} \sum \frac{1}{2\lambda+1} |a_{l\lambda m}(v'v)|^2 . \tag{5.6}$$

(The formulas involving the sum-averaging over j states are the ones which are presently useful in comparison with experiment in e-N_2 scattering, because the rotational spacing has not as yet been resolved.)

We now come to the fundamental statement of the hybrid-theory: *replace the adiabatic-nuclei matrix elements, Eq. (5.3), by the corresponding close-coupling values, Eq. (4.20), for whatever partial waves are necessary*:

$$a_{l\lambda m}(v', v) \to a^{(m)}_{v'l,v\lambda} . \tag{5.7}$$

(An equivalent replacement can be made for T and K matrices also.) The justification for this replacement we hope is clear. The point we wish to reemphasize is that the time delay criterion can be theoretically (and need not be experimentally) assessed. [It should be added, however, that any such criterion is always approximate in the sense that constant of proportionality is necessarily somewhat ambigous. In addition, in the present case the $R_0 = 2.068$ curve lies slightly removed from the main portion of the wave function $\chi_{v=0}(R)$ of the zero vibrational function of the N_2 molecule. Thus the theoretical nature of the time delay criterion must be understood within the confines of such mundane considerations.]

Coming back to the hybrid theory, note that the purely rotational aspects of even this Π_g wave are described by vector coupling coefficients which derive from the adiabatic-nuclei theory. It is this fact which has motivated us to call this a hybrid theory. One could in principle also include rotational close coupling at the same time as vibrational close coupling (cf. Sec. VI). Indeed Henry[30] has attempted that in the case of e-H_2 scattering with only limited success. The point is that the adiabatic-nuclei theory is quite sufficient,[28,31-34] when polarization is included, to explain the experimental data whereas vibrational-rotational close coupling even in the simpler e-H_2 case poses con-

vergence problems of a most serious nature, and it still does not include the main effects of polarization, which—in a close-coupling sense—would require higher-lying electronic states as well.

The adiabatic-nuclei amplitudes were calculated from the fixed-nuclei amplitudes (the eigenphases of which are those exemplified in Table I) using N_2 vibrational functions given by Herman and Wallis.[35] The $a_{l_i l_j m}(R)$ were interpolated, and a fifteen-point Gaussian quadrature was used to evaluate integral (5.3). (The j dependence of the vibrational functions in Ref. 35 was surpressed by setting $j=0$.) All of these non-Π_g amplitudes were combined with the amplitudes $a^{(m)}_{v'l,v\lambda}$ for the Π_g wave ($m=1$, even parity) from the close-coupling part of the calculation according to the hybrid-theory prescription above for the particular v and v' given in the results below.[36]

In Fig. 7 we give the total scattering cross section,

$$\sigma_T=\sum_{v'}\sigma_{v',0}=\sum_{v'}\frac{k_{v'}}{k_v}A_0(v',0)\,.$$

This cross section is mainly dominated by the vibrationally elastic scattering ($v'=0$), although the

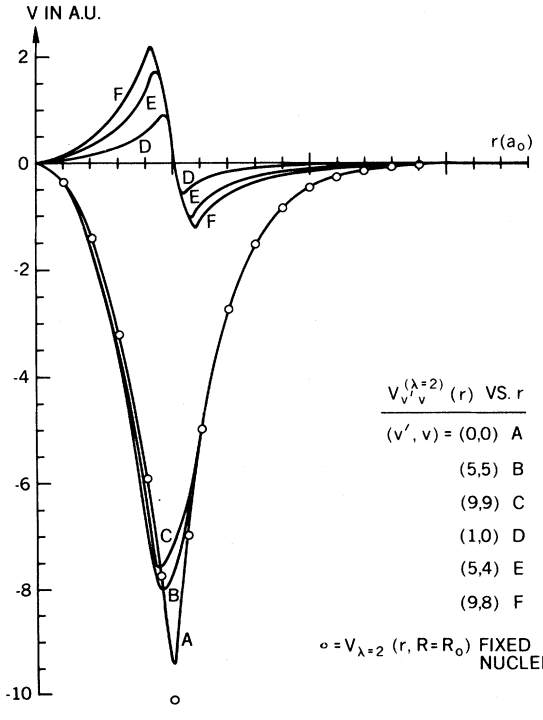

FIG. 3. Some diagonal and nondiagonal potentials of the vibrational close-coupling equations vs r. The corresponding fixed-nuclei potential is indicated by open circles.

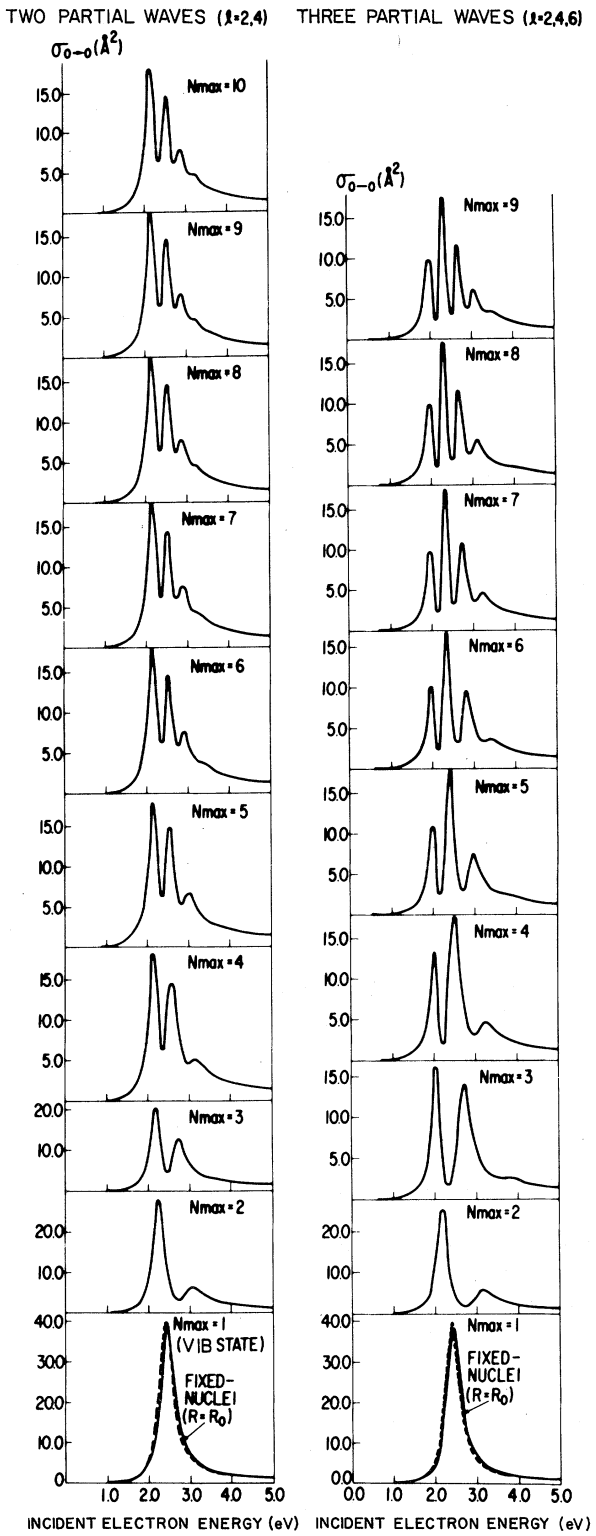

FIG. 4. Π_g contribution to the vibrationally elastic cross section σ_{00} including two- and three-partial waves for increasing number of vibrational states included in the close-coupling expansion.

valleys between the peaks are filled in significantly by the inelastic contributions (see below). Of prime significance is the fact that both the gross structure and substructure of the experiment,[7] given in the inset, are accounted for. In detail we see that the absolute cross sections of the first two maxima are about 40 and 25% above the experimental values, respectively; thereafter the agreement in shape and magnitude is very good. There tends to be a gradual shift of the calculated structure to larger energies as compared to experiment. That is clearly due to a lack of sufficient l coupling in the calculation as exemplified in Fig. 4. Whether all the discrepancies are due to deficiencies in the calculation is not so clear to us—in particular, the absolute magnitudes. It would be highly desirable to have independent experimental measurements of absolute magnitudes not only of the total but of the vibrationally elastic and inelastic cross sections as well. The theoretical curve does not give any structure below the first peak at 1.9 eV. Ehrhardt and Willmann[11] have found smooth behavior here also, so that the older experimental below 1.8 eV would appear to be spurious (cf. added note in Fig. 7 caption).

We next turn to differential cross sections involving vibrationally elastic scattering. This is the first case we encounter cross-term effects in the hybrid theory between resonant (calculated with close coupling) and nonresonant (calculated by adiabatic-nuclei theory) partial waves. That both cross-term and quadratic effects are important can be seen by comparing Fig. 8 with Fig. 9. Figure 8 gives the completely calculated differential cross sections including nonresonant waves for three of the energies measured by Ehrhardt and Willmann[11] (which results are given in the inset). In Fig. 9 similar results including only the Π_g partial wave are given. Not only are the latter spuriously symmetric about 90°, but the rise around 90° is completely absent both from the experiment and the full calculation. In Fig. 10 the full calculation is given for the remaining three measured energies (given in the inset). Note again that the calculation gives absolute values, but only the relative values are measured.[11] The shapes appear in satisfactory accord with experiment.[11]

The last comparison we shall give for vibrationally elastic scattering is the differential cross section as a function of the energy at various angles (Fig. 11). We consider the comparison very satisfactory, but the absence of the higher wiggles particularly, in the forward directions (due to the lack of sufficient coupling in the calculation as explained above) is somewhat more apparent than in the integral cross section (Fig. 7).

We turn next to the inelastic cross sections. In Figs. 12 and 13 we give the differential values at $\theta' = 20°$, 72° vs. k^2, respectively, these being the measurements in Refs. 11 and 6, respectively. In particular Schulz[6] inferred that his measurements would reflect the integrated cross sections as well. That this is so is shown in Fig. 14 where the integrated cross sections are given and are seen virtually indistinguishable from the 72° curve in shape. On the other hand the absolute values which were originally inferred by Schulz[6] on the basis of summed total cross sections measured by Haas[37] are about a factor of 2 smaller than his present estimate (cf. Fig. 14 caption).

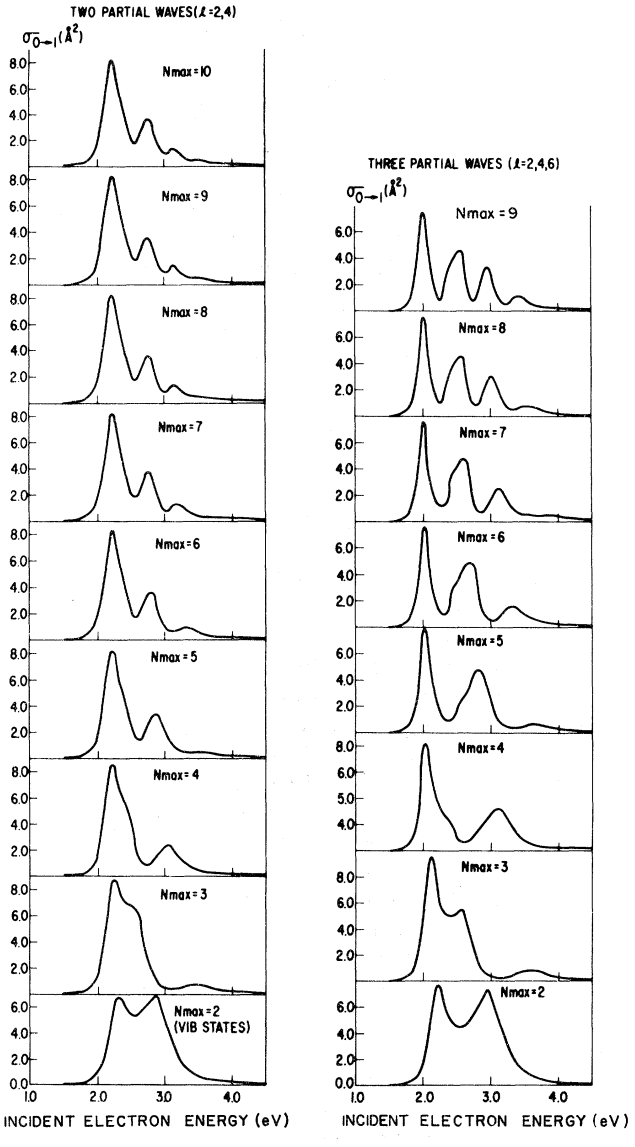

FIG. 5. Same as Fig. 4 but for $\sigma_{0\to1}(\equiv\sigma_{10})$.

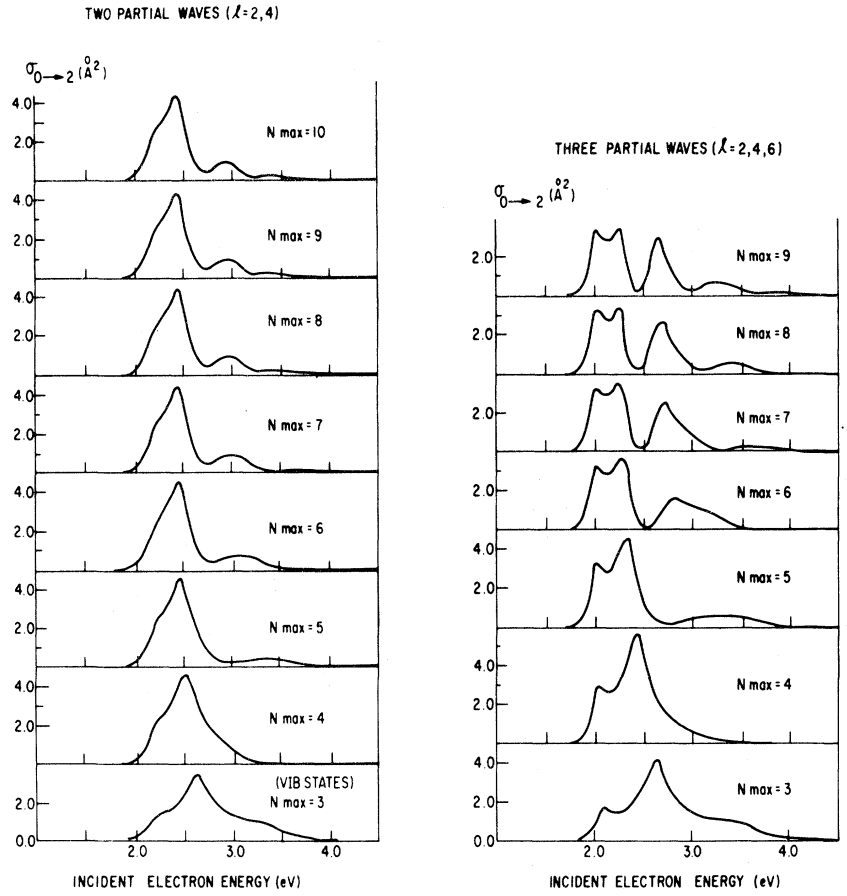

FIG. 6. Same as Fig. 4 but for $\sigma_{0\to 2}(\equiv\sigma_{20})$.

Thus the need for direct absolute measurements is clear, not only to test the theory but for many atmospheric applications, of which Ref. 1 is one, as well. Although the shape for the inelastic $v=0 \to v'=1$ cross section is satisfactory, the detailed agreement rapidly degenerates for higher v', and again this can be attributed to inadequate v and l coupling as noted in going from Fig. 4 to Fig. 6. We believe however that the average magnitudes of the particular cross sections are meaningful for practical applications.

It should be noted that, because of the virtual independence of the nonresonant amplitudes on R, essentially all of the inelastic cross sections comes from the resonant Π_g wave. This can be clearly seen in the inelastic-differential cross sections, given in Fig. 15, which are quite symmetric about 90°. Although the measurements of Ehrhardt and Willmann[11] are not done over sufficiently wide angular range to prove the symmetry, the agreement with calculation in terms of ratios of forward to minimum and 90° values at the different energies is very good.

Finally we give the momentum-transfer cross section. The formula for this cross section

$$\sigma_M \equiv \int \frac{d\sigma}{d\Omega'}(1-\cos\theta')\,d\Omega' \tag{5.8a}$$

is readily integrated from (5.4) to give

$$\sigma_M = \frac{\pi}{R^2}\sum_{v'}\left[A_0(v',0) - \tfrac{1}{3}A_1(v',0)\right], \tag{5.8b}$$

where the $A(v',0)$ are given in (5.4b) with the Π_g amplitudes replaced again by the close-coupling amplitudes according to the prescription (5.7) of the hybrid theory. [Note the $A_1(v',0)=0$ for $v'>0$ for Π_g.] The result of the calculation is compared with the experiment[38] in Fig. 16. The experiment as is well known does not measure σ_M directly, but rather infers it by optimizing assumed momentum transfer cross sections to fit swarm data as function of applied electric field. As such the absence of substructure on the "experimental" result should

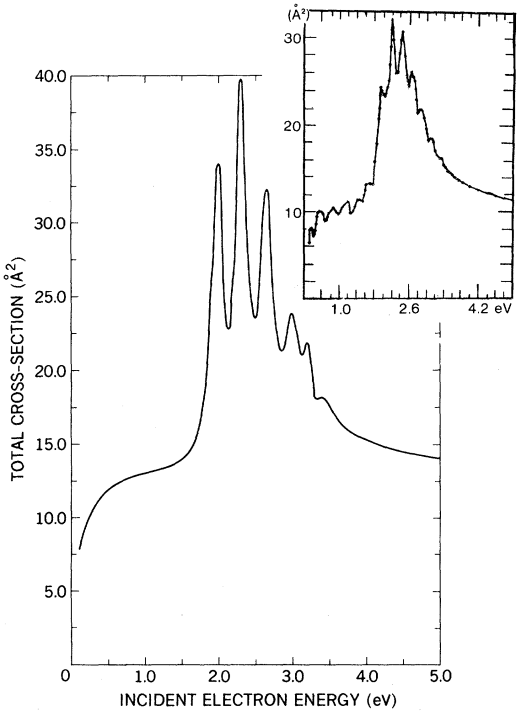

FIG. 7. Total scattering cross section in the full hybrid theory. Inset, experimental results of Golden (Ref. 7). In Ref. 11 the experimental structure below 1.8 eV is not found and is considered to be spurious. [*Note added in proof.* Golden (private communication) has suggested that his low-energy structure may be due to resonant superelastic collisions with vibrationally excited N_2 present in his target gas. Our calculation assumes all N_2 is initially in the ground vibrational state.]

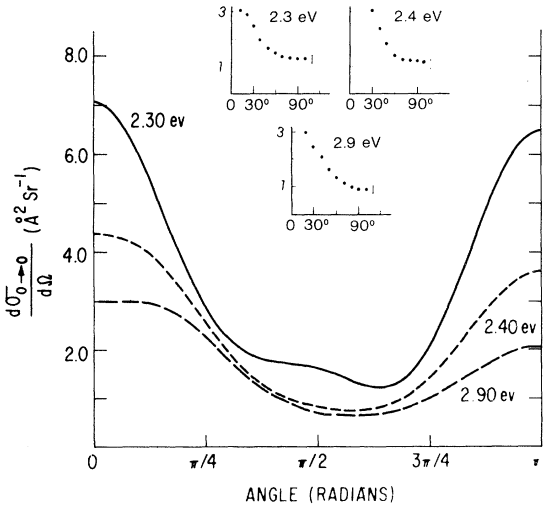

FIG. 8. Full hybrid theory calculation of vibrationally elastic differential cross sections at three energies. Inset, experimental results of Ehrhardt and Willmann (Ref. 11). Note ordinates of all angular *measurements* here and below are *relative*, not absolute, values.

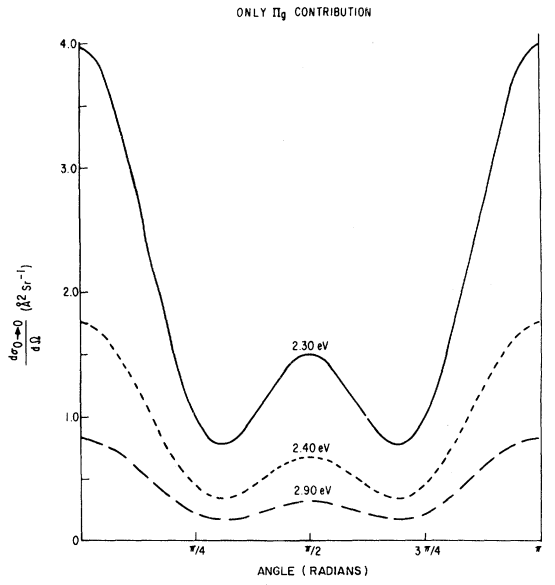

FIG. 9. Π_g contribution to $d\sigma_{00}/d\Omega$. Note the symmetry and enhancement around 90° are not present in the full calculation or the experiment; cf. Fig. 8.

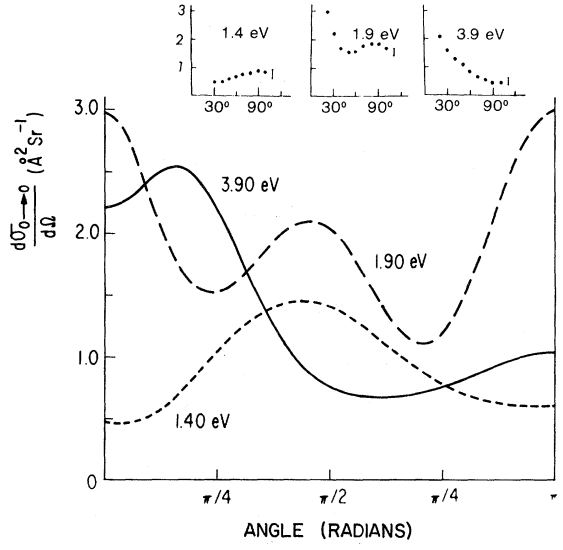

FIG. 10. Full hybrid-theory calculation of $d\sigma_{00}/d\Omega$ at remaining three energies measured in Ref. 11 which are given in inset.

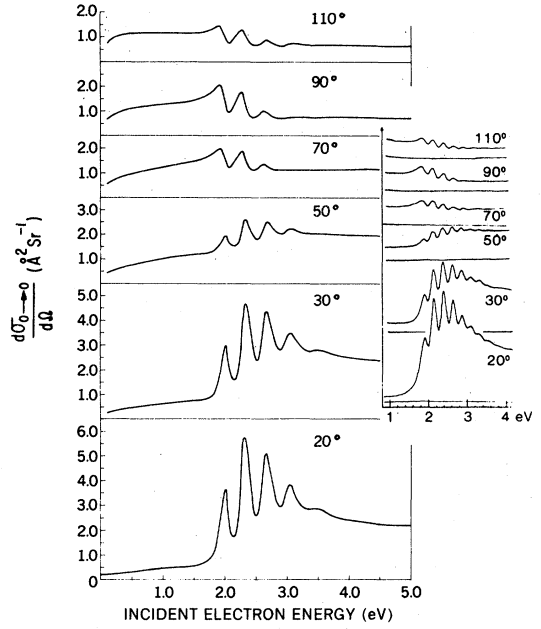

FIG. 11. $d\sigma_{00}/d\Omega$ vs k^2 for various angles. Experimental result of Ref. 11 given in inset.

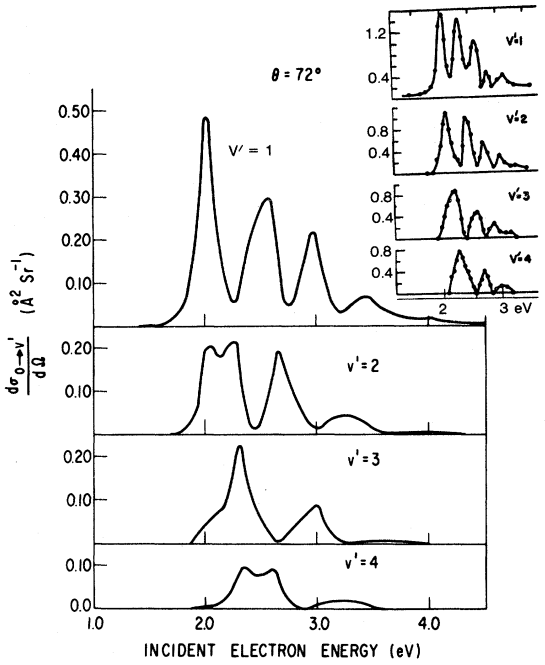

FIG. 13. Same as Fig. 12 for $\theta = 72°$. In this case the experimental result (inset) is that of Schulz, second paper of Ref. 6. The ordinate of the inset shows the original inferred normalization; cf. caption of Fig. 14.

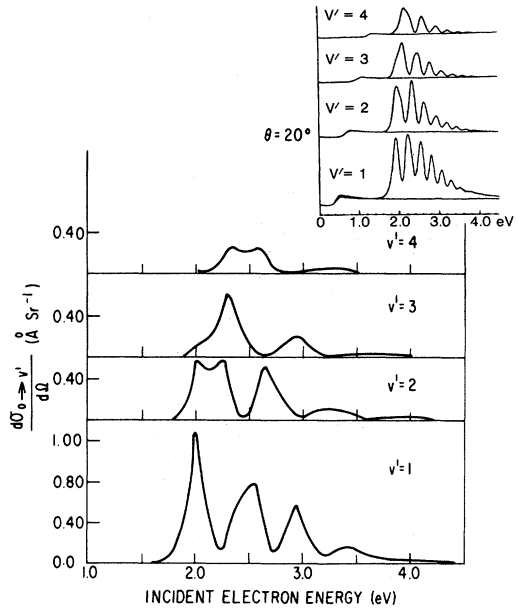

FIG. 12. $d\sigma_{0\to v}/d\Omega$ at $\theta = 20°$ for various excited states. Experimental results of Ref. 11 given in inset.

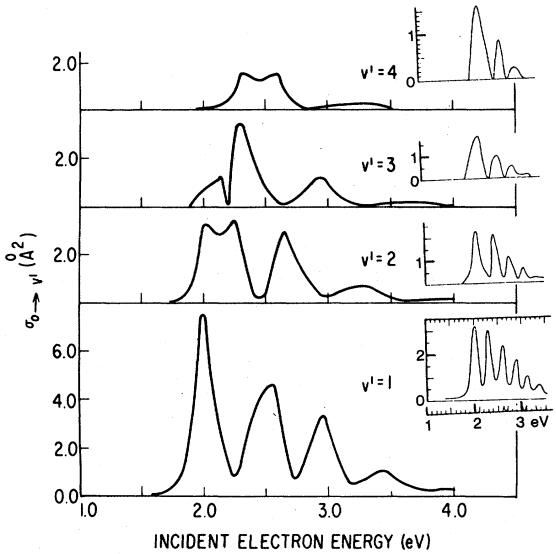

FIG. 14. Total vibrational excitation curves. Note similarity of shape to $\theta = 72°$ curves Fig. 13 as assumed by Schulz (Ref. 6, 1964), from which the experimental result is taken. The experimental normalization however is a factor of 2 higher than given in Ref. 6 and constitutes a new inferred normalization [Schulz (unpublished)]. In the latter, Schulz states that the new normalization may itself be low by a factor of 2, which is in accord with our results.

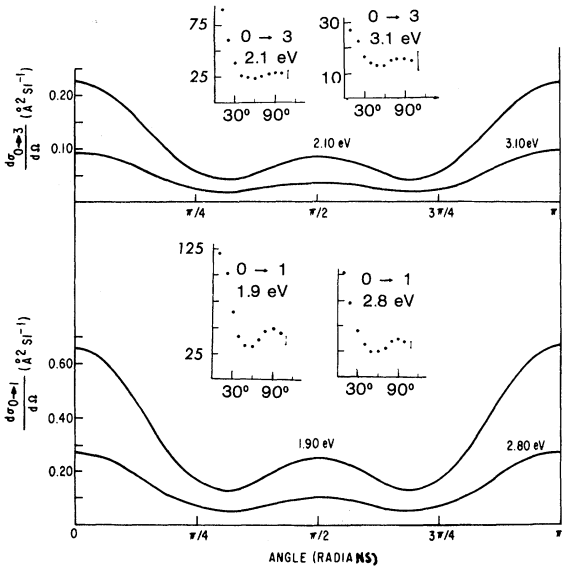

FIG. 15. Vibrationally inelastic differential cross sections compared to experiment (Ref. 11), inset. Note that the symmetry of the inelastic cross sections around 90° due to minuteness of non-Π_g contribution in these cases.

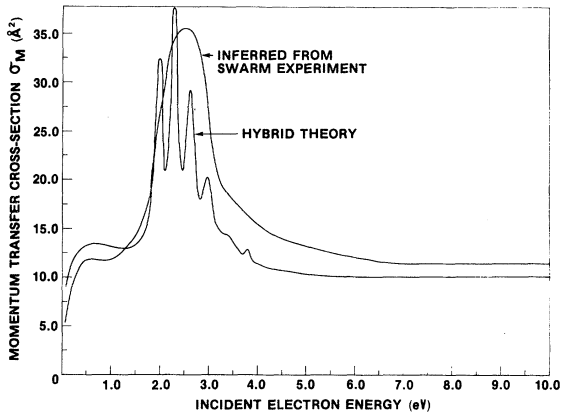

FIG. 16. Momentum-transfer cross section compared to the one inferred from swarm experiment by Englehardt, Phelps, and Risk (Ref. 38).

not be interpreted as its absence in fact. (It is virtually certain that the substructure must be present.) The experimental curve is seen to envelope the calculated curve in the resonance region as would be expected. About 25% of the calculated curve comes from the $v'>0$ terms in (5.8b). However the contribution of the resonances does not extend beyond about 4 eV, thus the 20% difference in this energy range would appear at this point to remain unexplained.

Finally it is clear from (5.2) and (5.7) that the hybrid theory can be used to calculate simultaneous rotation-vibration excitation. We shall not do that here as the programming of the formulas is somewhat more arduous, and there are presently no experiments with which to compare. (We do intend to perform that calculation at a later time.)

VI. DISCUSSION

This then completes our hybridization of vibrational close-coupling and adiabatic-nuclei rotational approximations. In order to complete the *a priori* theoretical framework for calculation of very narrow (probably Feshbach) resonances one will have to include rotational coupling as well. In that case the hybridization will take place at the second level only; i.e., the rotational and vibrational close-coupling amplitudes for the resonant partial wave will be merged with the adiabatic-nuclei amplitudes for the nonresonant partial wave. We expect to elucidate the formal aspects of this generalization shortly.

Calculations involving this generalized hybrid theory will certainly be arduous. It may well be that for practical purposes other techniques (R matrix, Fredholm determinant, etc.) may be more useful. But to be reliably accurate they will have to include the equivalent physics of the hybrid theory.

The frame-transformation theory[39,40] represents a different mix of the above theories. There one ties interior fixed-nuclei calculations to exterior close-coupling calculations at a boundary point r_0 utilizing appropriate simplifications for each region. The approach has undoubted utility in molecular photoionization and electron-molecular ion scattering, where the known asymptotic Coulomb solutions can be combined with multichannel quantum-defect theory[41] to render the resonant structure to be described in terms of a few experimental parameters.[39] It should be noted, however, that even here the fixed- and adiabatic-nuclei theories can describe the nonresonant structure very well.[42]

In the case of scattering from heteronuclear molecules (i.e., those with a dipole moment) frame-transformation can be expected to be useful[43] if for no other reason than rendering certain cross section finite which would diverge in the fixed- and adiabatic-nuclei approximations.[44] However, in the case of homonuclear diatomic molecules the utility of frame transformation is more uncertain, because the forces are probably not long-range enough to allow cross section to emerge which are suitably insensitive to the matching radius r_0.

ACKNOWLEDGMENTS

We are most grateful to Edward Sullivan for programming the adiabatic-nuclei part of this calculation. Assistance in the early stages of this investigation by Dr. Louis Wijnberg is appreciated.

---

*NRC-NASA Resident Research Associate.

[1]G. P. Newton, J. C. G. Walker, P. H. E. Meijer, J. Geophys. Res. 79, 3807 (1974); G. P. Newton and J. C. G. Walker, *ibid.* (to be published).

[2]For a review of the experimental results see G. J. Schulz, Rev. Mod. Phys. 45, 423 (1973).

[3]See *Molecules in the Galactic Environment*, edited by M. A. Gordon and L. E. Snyder (Wiley, New York, 1973).

[4]For a review of the fixed- and adiabatic-nuclei theories (plus other theory and experiment) cf. D. E. Golden, N. F. Lane, A. Temkin, E. Gerjuoy, Rev. Mod. Phys. 43, 642 (1971).

[5]P. G. Burke and N. Chandra, J. Phys. B 5, 1696 (1972).

[6]G. J. Schulz, Phys. Rev. 125, 229 (1962); 135, A988 (1964).

[7]D. E. Golden, Phys. Rev. Lett. 17, 847 (1966).

[8]A. Herzenberg and F. Mandl, Proc. R. Soc. Lond. A 270, 48 (1962). For a review of the Kapur-Pierls and Siegert formalisms, which is the basis of the work of this group, cf. J. N. Bardsley and F. Mandl, Rep. Prog. Phys. 31, 471 (1968).

[9]J. C. Y. Chen, J. Chem. Phys. 40, 3507, 3515 (1964), 45, 2710 (1966); Phys. Rev. 146, 61 (1966). The penultimate reference contains the first explanation of the movement of peak positions with vibrational quantum number. In this context cf. also A. Herzenberg, J. Phys. B 1, 548 (1968) and Ref. 10.

[10]D. T. Birtwistle and A. Herzenberg, J. Phys. B 4, 53 (1971).

[11]H. Ehrhardt and K. Willmann, Z. Phys. 204, 462 (1967).

[12]M. Krauss and F. H. Mies, Phys. Rev. A 1, 1592 (1970).

[13]F. R. Gilmore, J. Quant. Spectrosc. Radiat. Transfer 5, 369 (1965).

[14]P. G. Burke and A. L. Sinfailam, J. Phys. B 3, 641 (1970).

[15]A. Temkin and K. V. Vasavada, Phys. Rev. 160, 109 (1967).

[16]A. Temkin, K. V. Vasavada, E. S. Chang, and A. Silver, Phys. Rev. 186, 57 (1969).

[17]R. K. Nesbet, J. Chem. Phys. 40, 3619 (1964).

[18]F. H. M. Faisal and A. L. Tench, Comput. Phys. Commun. 2, 261 (1971).

[19]R. M. Sternheimer, Phys. Rev. 96, 951 (1954).

[20]D. G. Truhlar, Phys. Rev. A 7, 2217 (1973).

[21]Equation (2.5) of Ref. 5 contains a typographical error; the imaginary factor should be $i^{l'-l}$. This is correctly reflected in our formula (3.14).

[22]N. Chandra, Comput. Phys. Commun. 5, 417 (1973).

[23]A. Temkin, in *Fundamental Interactions in Physics*, edited by B. Kursunoghu and A. Perlmutter (Plenum, New York, 1973), Vol. 2, pp. 298ff.

[24]A. Herzenberg in the volume cited in Ref. 23, pp. 261 ff., has argued against the adiabatic-nuclei theory on the basis that the substructure of the Π_g resonance has a width comparable to the vibrational spacing of N_2. The argument is correct, but it depends on observation and therefore does not suffice for the needs of a predictive calculational method.

[25]Vector coupling coefficients are in the form 3-j and 6-j symbols. For definitions, notation, and formulas see A. R. Edmonds, *Angular Momentum in Quantum Mechanics* (Princeton U. P., Princeton, N. J., 1957).

[26]D. M. Chase, Phys. Rev. 104, 838 (1956).

[27]A. Temkin and F. H. M. Faisal, Phys. Rev. A 3, 520 (1971).

[28]E. Chang and A. Temkin, Phys. Rev. Lett. 23, 399 (1969).

[29]This represents the first time the adiabatic-nuclei formulas for simultaneous-rotation excitation has been given explicity in full nondiagonal form. In the diagonal approximation the formulas are given in Refs. 32 and 34.

[30]R. J. W. Henry, Phys. Rev. A 2, 1349 (1970).

[31]S. Hara, J. Phys. Soc. Jpn. 27, 1592 (1969).

[32]F. H. M. Faisal and A. Temkin, Phys. Rev. Lett. 28, 203 (1972).

[33]R. J. W. Henry and E. S. Chang, Phys. Rev. A 5, 276 (1972).

[34]A. Temkin and E. Sullivan, Phys. Rev. Lett. 33, 1057 (1974).

[35]R. Herman and R. F. Wallis, J. Chem. Phys. 23, 637 (1955).

[36]Results for transitions to yet higher v' states from several $v \geq 0$ states, needed for example in SAR problem, Refs. 1, will be compiled by the authors in the form of a NASA Technical Note (unpublished).

[37]R. Haas, Z. Phys. 148, 177 (1957). A transmission experiment for inelastic vibrational excitation was also carried out by J. B. Hasted and A. M. Awan, J. Phys. B 2, 367 (1969), with results similar to those of Schulz, Ref. 6.

[38]A. M. Englehardt, A. V. Phelps, C. G. Risk, Phys. Rev. 135, A1566 (1964).

[39]U. Fano, Comments At. Mol. Phys. 2, 47 (1970); Phys. Rev. A 2, 353 (1970).

[40]E. S. Chang and U. Fano, Phys. Rev. A 6, 173 (1972).

[41]M. J. Seaton, Proc. Phys. Soc. Lond. 88, 801 (1966).

[42]E. S. Chang and A. Temkin, J. Phys. Soc. Jpn. 29, 172 (1970).

[43]N. Chandra and F. A. Gianturco, Chem. Phys. Lett. 24, 326 (1974).

[44]W. R. Garrett, Mol. Phys. 24, 465 (1972).